

Cyclosporine Immunomodulation Retards Regeneration of Surgically Transected Corneal Nerves

Abed Namavari, Shweta Chaudhary, Jin-Hong Chang, Lisette Yco, Snehal Sonawane, Vishakha Khanolkar, Beatrice Y. Yue, Joy Sarkar, and Sandeep Jain

PURPOSE. To determine whether immunomodulation with cyclosporine (CsA) affects reinnervation after surgical transection of stromal nerves.

METHODS. *Thy1*-YFP+ neurofluorescent mice underwent lamellar corneal surgery and 3 days later, received artificial tears or CsA eye drops for 6 weeks. Serial in vivo wide-field stereofluorescent microscopy was performed to determine changes in nerve fiber density (NFD). Real-time quantitative PCR was performed to determine the expression of neurotrophins and cytokines (IL6 and TNF- α). Compartmental culture of trigeminal ganglion neurons was performed in Campenot devices to determine whether CsA directly affects neurite outgrowth.

RESULTS. Yellow fluorescent protein (YFP)-positive cells significantly increased at 3 and 7 days after surgery. The number of YFP-positive cells in the cornea was significantly lower in the CsA group than that in the control group. The percentage increase in NFD between 2 to 6 weeks was greater in the control group (80% \pm 10%, $P = 0.05$) than that in the CsA group (39% \pm 21%). The CsA group also exhibited lower expression of IL6 and TNF- α ($P = 0.01$). In compartmental culture experiments, neurite outgrowth toward side compartments containing CsA was significantly less (2.29 \pm 0.4 mm, $P = 0.01$) than that toward side compartments containing vehicle (3.97 \pm 0.71 mm).

CONCLUSIONS. Immunomodulation with CsA reduces the expression of cytokines (IL6) in the cornea and retards regenerative sprouting from transected corneal stromal nerve trunks. In addition, CsA has a direct growth inhibitory action on neurites as well. (*Invest Ophthalmol Vis Sci.* 2012;53:732-740) DOI: 10.1167/iops.11-8445

Neurotrophins, regeneration-associated genes, and the presence of inflammation are factors demonstrated to affect regeneration of injured nerves.¹⁻³ The emerging view regarding inflammation is that it may not be deleterious to regenerating nerves. Rather, it may have beneficial effects that preserve injured neurons and promote regeneration. In the

literature, contrasting results have been reported regarding the neuroprotective effect of inflammation.^{4,5} Schwartz et al.⁶ reported that T-lymphocytes are neuroprotective after spinal cord crush injury, whereas Jones et al.⁷ reported that T cells exacerbate neuropathology after spinal cord injury. In the skin, evidence suggests that inflammatory conditions are associated with increased nerve innervation.⁸

In the cornea, specific cellular and molecular factors control inflammation, promote resolution, and afford neuroprotection.⁹ The cornea is densely innervated with nerves that terminate as free nerve endings. Although inflammation forms the pathophysiologic basis of many corneal disorders, the connection between corneal inflammation and nerve regeneration is largely unknown. Whether the inflammatory response is beneficial or detrimental to the corneal nerves, especially regenerating ones, is unclear. Data published so far have been conflicting with regard to corneal nerve density in eyes with underlying inflammation such as that seen in dry eye disease. Zhang et al.¹⁰ observed increased subbasal nerve counts in patients with dry eye and tear deficiency, whereas decreased nerve counts were noted by Benítez-del-Castillo et al.^{11,12} and Villani et al.¹³ Tuisku et al.¹⁴ and Tuominen et al.¹⁵ reported that, in patients with Sjögren syndrome, the corneal subbasal nerve exhibits abnormal nerve growth cone-like patterns and nerve sprouting, features suggestive of nerve regeneration. Various mechanisms have been proposed to explain the beneficial effect of inflammation on corneal nerve regeneration. Infiltrating T cells, neutrophils, and platelets promote nerve regeneration.¹⁶ Inflammatory cytokines in the tears have also been reported to promote nerve regeneration.¹⁷⁻¹⁹

Here, we investigated whether immunomodulation with cyclosporine (CsA), an anti-inflammatory drug, affects reinnervation after transection of corneal stromal nerves. Lamellar corneal surgery was performed in *thy1*-YFP+ mice, which express yellow fluorescent protein (YFP) under the direction of the promoter *thy1*, which is not only a pan T-cell marker in mice but also a neuronal marker.^{20,21} Therefore, *thy1*-YFP+ mice allow for simultaneous visualization of inflammatory cells and nerve fibers. To complement these in vivo studies, we performed compartmental culture of trigeminal ganglion cells to determine whether CsA has a direct effect on axonal growth in addition to its immunomodulatory actions.

METHODS

Animals

All animals were managed and experiments were conducted according to the ARVO Statement for the Use of Animals in Ophthalmic and Vision Research. The animal protocol was approved by the Animal Care Committee of the University of Illinois at Chicago. Neurofluorescent homozygous adult mice (6-8 weeks old) of the *thy1*-YFP line were purchased from a commercial supplier (Jackson Laboratories, Bar Harbor, ME). For in vivo experiments, mice were anesthetized with

From the Corneal Neurobiology Laboratory, Department of Ophthalmology and Visual Sciences, University of Illinois at Chicago, College of Medicine, Chicago, Illinois.

Supported in part by National Institutes of Health/National Eye Institute Grants EY018874 (SJ) and Core Grant EY001792 (DA) and an unrestricted grant from Research to Prevent Blindness, Inc., New York, NY.

Submitted for publication August 18, 2011; revised December 8, 2011; accepted December 16, 2011.

Disclosure: A. Namavari, None; S. Chaudhary, None; J.-H. Chang, None; L. Yco, None; S. Sonawane, None; V. Khanolkar, None; B.Y. Yue, None; J. Sarkar, None; S. Jain, None

Corresponding author: Sandeep Jain, Department of Ophthalmology and Visual Sciences, University of Illinois at Chicago, 1855 W. Taylor Street, Chicago, IL 60612; jains@uic.edu.

intraperitoneal injections of ketamine (20 mg/kg; Phoenix Scientific, St. Joseph, MO) and xylazine (6 mg/kg; Phoenix Scientific). For terminal experiments, mice were euthanized according to the animal care committee protocol. Animals were excluded from the study and euthanized if, at any point, they developed corneal neovascularization or opacity.

Animal Surgery

Surgery was performed on the left eye of each animal. The central cornea was marked with a 2-mm-diameter disposable trephine (VisiPunch; Huot Instruments, Menomonee Falls, WI). A partial-thickness incision, 0.2 mm in length, was made perpendicular to the corneal surface and tangential to the circular trephine mark using a 15°, 5.0-mm standard angle knife (iKnife model 8065401501; Alcon, Fort Worth, TX). The peripheral lip of the corneal incision was depressed to penetrate the stroma centripetally, creating a corneal pocket. A 1.0-mm paracentesis knife (ClearCut Sideport model 8065921540; Alcon) was used to expand the corneal pocket to the 2-mm-diameter trephine mark. Next, a 45°, 1.75-mm subretinal spatula (Grieshaber UltraSharp model 682.11; Alcon) was used to enter the corneal pocket, incise it from within, and exit out at the 2-mm-diameter trephine mark. Micro spring-open scissors (Vannas) were then used to extend the circumferential incision along the trephine mark. At three points (each approximately 0.5 clock hours), the corneal pocket was left unincised. This formed three hinges that allowed the flap to remain attached to the cornea in the absence of sutures. Animals received antibiotic ointment in the eye and underwent suture tarsorrhaphy, which was opened after 3 days. Brightfield images were taken to ensure corneal clarity over the course of the study.

Lamellar corneal flap surgery was performed in 18 mice. Animals were subsequently divided randomly into treatment and control groups (9 mice per group). One mouse was excluded from each group because of corneal scarring ($n = 1$) or neovascularization ($n = 1$). Starting 3 days after surgery, animals received 7 μ L of 0.05% CsA eye drops (Restasis; Allergan, Irvine, CA) or artificial tears (Optive; Allergan) twice daily for 6 weeks. Serial *in vivo* nerve imaging was performed at baseline and at 2-week intervals for 6 weeks.

In Vivo Stereofluorescent Microscopic Imaging

Serial imaging was performed using a fluorescence stereomicroscope (StereoLumar V.12; Carl Zeiss Microscopy, Thornwood, NY) equipped with a digital camera (AxioCam MRm; Carl Zeiss) and software (Axiovision 4.0). An anesthetized mouse was placed on the stereoscope stage, after which 7 μ L of proparacaine (0.5%; Bausch & Lomb, Tampa, FL) was applied for 3 minutes and the pupil was constricted with 0.01% carbamylcholine (Carbachol, Miostat; Alcon) for 5 minutes. Z-stack images were obtained at 5- μ m intervals and compacted into one maximum intensity projection (MIP) image after alignment (Zeiss Axiovision software). Nerve fibers were traced manually using neuron reconstruction, 3D mapping software (NeuroLucida; MBF Bioscience, Williston, VT). For time course studies, corresponding points on the images from different time points were selected to make a contour, and nerve tracing was performed within the contour area. A neurophysiologic data analysis software package (NeuroExplorer; Nex Technologies, Littleton, MA) was used to measure the total length of fibers and the area of the contour in which nerves had been traced. Corneal nerve fiber density (NFD) was calculated by dividing the total length of nerve fibers (mm) with the area of the contour (mm^2) as described by Al-Aqaba et al.²²

Corneal Whole-Mount Immunostaining

Excised corneas were processed for whole-mount immunofluorescence staining. Corneas were fixed in 4% paraformaldehyde overnight at 4°C, and washed four times with PBS (for 15 minutes each). Corneas were then permeabilized and blocked overnight at 4°C in 1% Triton X-100, 1% bovine serum albumin, and 10% normal donkey serum in PBS. The corneas were incubated in primary antibody diluted in the

blocking solution (1:100) for 48 hours at 4°C, washed four times in PBS (for 15 minutes each), and incubated with secondary antibody diluted in the blocking solution (1:350) overnight at 4°C. Corneas were further washed and mounted in mounting medium on glass slides. Primary antibody was purified hamster anti-mouse $\gamma\delta$ T-cell receptor (cat. #553175; BD Pharmingen, San Diego, CA). The specificity of this antibody has been established in murine tissue.¹⁶ Secondary antibody was commercial conjugated donkey anti-hamster IgG (Dylight 594 AffiniPure; Jackson ImmunoResearch, West Grove, PA), which was chosen to ensure nonoverlap with the YFP wavelength and to minimize false-positive staining. The nuclei were stained with 4',6'-diamidino-2-phenylindole (DAPI). Primary antibody was omitted for negative control. Z-stack images of corneal whole-mounts were obtained using a confocal microscope (LSM 510 META; Carl Zeiss GmbH, Hamburg, Germany).

Isolation, Culture, and Immunostaining of Corneal Stromal Cells

Murine corneal stromal cells were isolated using modified three sequential collagenase digestions as previously described.²³ The isolated cells were then cultured in keratocyte, fibroblast, or myofibroblast induction media. Keratocytes were cultured using Dulbecco's modified Eagle's medium nutrient mixture F12 (DMEM/F12) without serum. Fibroblasts were cultured in media with 10 ng/mL recombinant human fibroblast growth factor basic (R&D Systems, Minneapolis, MN). Myofibroblasts were cultured in media with 10 ng/mL recombinant human TGF- β 1 (R&D Systems). Immunostaining was performed as described earlier. Primary antibody was polyclonal rabbit anti- α -smooth muscle actin antibody (cat. #29553; AnaSpec, Fremont, CA). Secondary antibody was conjugated donkey anti-rabbit IgG (Dylight 594, AffiniPure; Jackson ImmunoResearch), as used earlier. The nuclei were stained with DAPI. Primary antibody was omitted for negative control.

Real-Time Quantitative PCR

At 6 weeks, corneas were harvested and expressions of neurotrophins and inflammatory cytokines were analyzed by real-time quantitative PCR (qPCR). At 6 days (1 day after exposure to CsA), cultured trigeminal neurons were harvested and the gene expression changes due to CsA exposure were analyzed by qPCR. PCR was performed using primers for nerve growth factor (NGF; cat. #PPM03596B; SABiosciences, Frederick, MD), brain-derived neurotrophic factor (BDNF; cat. #PPM03006B), neurotrophin 3 (NT3; cat. #PPM04325A), neurotrophin 5 (NT5; cat. #PPM04324A), glial cell line-derived neurotrophic factor (GDNF; cat. #PPM04315E), interleukin-6 (IL6, cat. #PM03015A), tumor necrosis factor- α (TNF- α ; cat. #PPM03113F), FBJ osteosarcoma oncogene (FOS; cat. #PPM02940B), nuclear factor of activated T cells, cytoplasmic, calcineurin-dependent 1 (NFATC1; cat. #PPM04560F), mitogen-activated protein kinase 14 (MAPK14; cat. #PPM03578A), and growth-associated protein 43 (GAP43; cat. #PPM03303A). The central cornea was marked with a trephine, incised with scissors, and placed directly in a commercial ready-to-use reagent (TRIzol; Invitrogen, Carlsbad, CA) for RNA extraction, which was conducted according to the manufacturer's protocol. Reverse transcription was performed with 50 ng total RNA using a commercial kit (RT² First Strand cDNA Synthesis Kit; SABiosciences). The resulting cDNA was preamplified using a commercial package (RT² Nano PreAMP Kit; SABiosciences) according to the manufacturer's instructions (12 cycles of 95°C for 15 seconds and one cycle of 60°C for 2 minutes). Real-time qPCR was performed with a nucleic acid cyanine stain (SYBR) using a real-time instrument (7900HT ABD). Samples were assayed in triplicate in a total volume of 25 μ L using thermal cycling conditions of 10 minutes at 95°C followed by 40 cycles of 95°C for 15 seconds and 60°C for 60 seconds. A mouse genomic DNA contamination control was used to confirm that DNA contamination did not occur in reagents used for amplification. For data analysis, the cycle threshold (CT) of each gene for the CsA-treated eye was normalized to the corresponding value for the artificial-tear-treated eye and then used to calculate the fold change with the $2^{-\Delta\Delta CT}$

method. For trigeminal cultures, the CTs for each gene in the CsA-exposed neurons were normalized to the corresponding value for freshly dissociated trigeminal neurons (control) and then used to calculate the fold change.

Trigeminal Ganglion Cell Culture

Trigeminal ganglia neurons were isolated from 10-day-old *thy1*-YFP pups and cultured as described by Malin et al.²⁴ Compartmental culture devices were assembled using a commercial divider (Teflon, modified CAMP3NS; Tyler Research Corp., Edmonton, Alberta, Canada) as described previously.^{25,26} Tracks were etched onto collagen-coated culture dishes to direct the neurite growth. On day 1, trigeminal neuronal cells (1×10^3) were plated in the central compartment and maintained in F12 media containing 10% fetal calf serum (FCS; Invitrogen), penicillin-streptomycin (Invitrogen), and NGF (10 μ g/mL; Biomedical Technologies, Stoughton, MA). The side compartments were filled with a mixture that was identical, except that it also contained cytosine arabinoside (AraC, 0.3 μ M; Sigma, St. Louis, MO) to inhibit the growth of glial cells.²⁷ On day 3, fresh media was added, with the media mixtures in the central and side compartments being reversed.

CsA Treatment of Trigeminal Ganglion Cultures

Cultures were treated with 5 μ g/mL CsA (Sigma) or vehicle (PBS) on day 5. The central compartment was filled with F12 media containing 10% FCS, penicillin-streptomycin, NGF (10 μ g/mL), and AraC (0.3 μ M), whereas the side compartments were filled with a mixture that was identical, except that it lacked AraC and contained CsA (5 μ g/mL). Cultures were incubated for 24 hours. The media in all compartments was then replaced with F12 supplemented with NGF (10 μ g/mL), and cells were cultured for an additional 24 hours. Therefore, neurites were exposed to CsA or vehicle for 24 hours, and the total time of neurite growth after intervention was 48 hours. The CsA concentration was selected based on studies by Gortzak et al.²⁷ and Chen et al.²⁸ Images of neurite outgrowth along tracks were acquired on day 5 and 48 hours after treatment (on day 7). All images were analyzed using neuron reconstruction, 3D mapping software (NeuroLucida; MBF Bioscience), as used earlier.

Analysis of Neurite Outgrowth in Trigeminal Ganglion Cultures

After 3 days of culture, neurites extended from cell bodies in the central compartment and crossed the divider (Teflon) to reach the tracks in the side compartment. Tracks in which neurite extended >750 μ m beyond the divider barrier were selected a priori on day 5, before any interventions. Only these tracks with robust neurite growth were included in the analysis. Nerve fiber length (NFL) was measured in each track using commercial neuron reconstruction software (AutoNeuron; MBF Bioscience). NFL was calculated on day 5 (before vehicle or CsA treatment) and on day 7 (after vehicle or CsA treatment). The increase in NFL between days 5 and 7 was determined. In vitro experiments were terminated on day 7. After removal of the media, the contents of the central and side compartments were collected in a commercial ready-to-use reagent (TRIzol) and processed for PCR.

Statistical Analysis

Statistical analyses were performed using a commercial data analysis spreadsheet software (Microsoft Excel). Student's *t*-test was used to compare mean values between groups. Differences were considered significant when $P < 0.05$.

RESULTS

Inflammatory Cell Influx after Lamellar Corneal Surgery

After lamellar corneal surgery, we observed an influx of YFP-positive cells in the cornea of *thy1*-YFP+ mice (Figs. 1B1–B3). Analysis of MIP images captured with a wide-field stereofluorescence microscope showed that the number of YFP-positive cells in the cornea was greater at postoperative day 3 (271 ± 71 , $P = 0.006$) and day 7 (61 ± 25 , $P = 0.03$) than before the operation (4.0 ± 0.8) (Fig. 1C). The YFP-positive cells decreased significantly between postoperative day 3 and day 7 ($P = 0.004$). The influx of YFP+ cells thus peaked at day 3 and regressed thereafter. Confocal microscopy revealed that the *thy1*-YFP+ cells (*thy1* is a pan T-cell marker in mice²⁰) were approximately 12 μ m in size (Fig. 1D1) with a large nucleus (Fig. 1D2) characteristic of bone marrow-derived cells of lymphoid lineage.

Using three-dimensional reconstruction of confocal microscopic images, we found that the YFP-positive cells were present in the anterior stroma of the peripheral cornea just outside the flap margin (Fig. 2A1) as well as in the anterior and posterior stroma of the central cornea over the flap (Fig. 2A2). The location of the posterior stromal YFP+ cells approximated the corneal flap/bed interface. The stained YFP+ cells ($\gamma\delta$ T-cell receptor antibody) (Figs. 2B1–B4), confirming that the YFP+ cells are of T-cell lineage. The DAPI-stained corneal stromal cells surrounding the YFP+ nerves and T cells did not show fluorescence. Cultured activated keratocytes (fibroblasts and myofibroblasts) also did not show YFP fluorescence. Fibroblasts (Figs. 2C1, C2) showed less α -smooth muscle actin staining compared with myofibroblasts (Figs. 2D1, D2), but both were not YFP fluorescent.

Effect of CsA Immunomodulation on In Vivo Nerve Regeneration

To understand whether CsA immunomodulation affects nerve regeneration, we measured NFD in *thy1*-YFP+ mice that had undergone lamellar corneal surgery and had been treated with either CsA or artificial tears (control) for 6 weeks. Serial in vivo fluorescence imaging was performed and MIP images were analyzed to calculate the NFD of corneas (Figs. 3A1–A4 and B1–B4). In the control group, the NFD increased from 13.4 ± 1.4 mm/mm² at 2 weeks to 23.7 ± 2.2 mm/mm² at 6 weeks. In the CsA group, the NFD was 12.5 ± 1.6 mm/mm² at 2 weeks and 15.8 ± 1.2 mm/mm² at 6 weeks. The change in NFD between weeks 2 and 6 was normalized to the 2-week NFD to calculate the percentage increase in NFD. This percentage increase was significantly greater in the control group ($80\% \pm 10\%$, $P = 0.05$) than that in the CsA group ($39\% \pm 21\%$) (Fig. 3C). Consistent with these findings, the number of YFP-positive cells in the cornea was lower in the CsA group than that in the control group at 2 weeks (2.1 ± 0.7 vs. 5.1 ± 1.3), 4 weeks (1.8 ± 0.4 vs. 5.4 ± 1.5), and 6 weeks (2.1 ± 0.6 vs. 5.9 ± 1.9) ($P < 0.05$) (Fig. 3D).

At 6 weeks, corneas were excised, pooled, and processed for PCR analysis of neurotrophins and inflammatory cytokines. Expression of NGF, BDNF, GDNF, and NT3 did not significantly differ between the two groups (Fig. 3E). However, NT5 expression was lower in the CsA group than that in the control group ($P = 0.03$) (Fig. 3E). The CsA group also exhibited markedly lower levels of the inflammatory cytokines, IL6 and TNF- α ($P = 0.01$) (Fig. 3F).

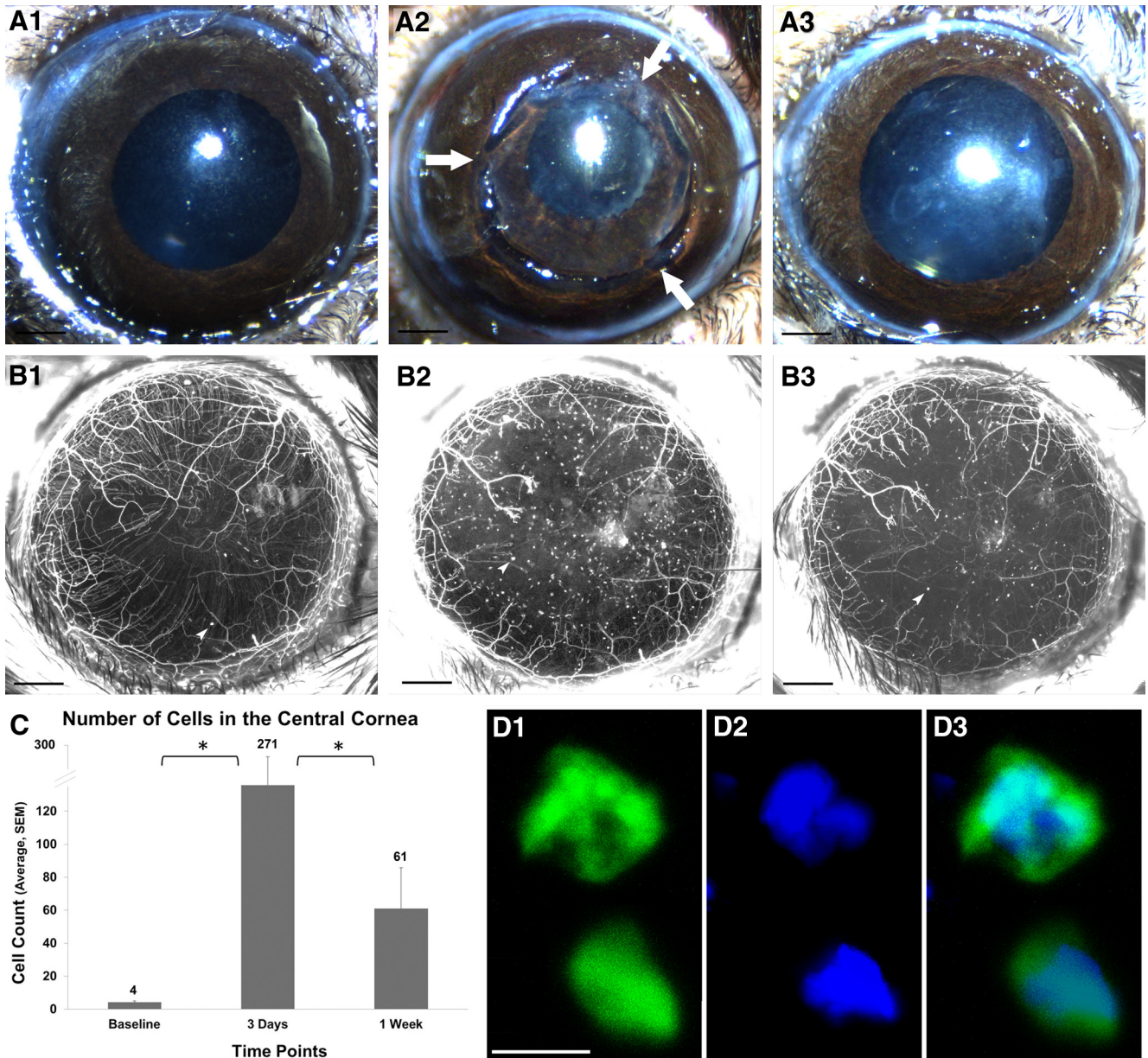


FIGURE 1. Inflammatory cell influx after lamellar corneal surgery. (**A1–A3**) Color images of a cornea before surgery (**A1**), immediately after surgery (**A2**; *arrows* point to flap hinges), and 1 week after surgery showing uncomplicated healing (**A3**). (**B1–B3**) In vivo maximum intensity projection image of fluorescent nerves and inflammatory cells in *thy1*-YFP mouse cornea before surgery (**B1**), 3 days after surgery (**B2**), and 1 week after surgery (**B3**). Black scale bar, 500 μm . *Arrowheads* point to YFP-positive inflammatory cells. (**C**) Quantification of YFP-positive cells, which peaked at day 3. * $P < 0.05$. (**D**) Confocal microscope image of *thy1*-YFP+ cells (*thy1* is a pan T-cell marker in mice²⁰). The nucleus is stained *blue* with DAPI. The YFP+ cells are approximately 12 μm in size (**D1**), with a large nucleus (**D2**) characteristic of bone marrow-derived cells of lymphoid lineage. White scale bar, 10 μm .

Effect of CsA Immunomodulation on In Vitro Nerve Regeneration

To investigate whether CsA has direct neuronal actions, we performed compartmental culture of dissociated trigeminal ganglion neurons and analyzed neurite outgrowth toward the side compartment containing 5 $\mu\text{g}/\text{mL}$ of CsA. We found that the neurite outgrowth (nerve fiber length/track) over a 48-hour period (between days 5 to 7) was less in the CsA group (0.04 ± 0.1 mm, $P < 0.001$) than that in the vehicle group (1.6 ± 0.3) (Fig. 4E). NFL at day 7 was significantly lower in the CsA group (2.29 ± 0.4 mm, $P = 0.01$) compared with the vehicle group (3.97 ± 0.71 mm), although at day 5 the NFL was similar between the two groups. At day 7, the axons from the side

compartment and the cell bodies from the central compartment were pooled and processed for PCR analysis of NGF, BDNF, GDNF, NT3, and NT5. Of these neurotrophins, only BDNF and NT5 differed between groups (Fig. 4F). Expression of both these factors was lower in the CsA group than that in the control group ($P = 0.01$ for BDNF and $P = 0.03$ for NT5).

To determine whether the effects seen on the neuronal growth and gene expression are due to the specific effects of CsA and not cytotoxicity, we analyzed the expression of NFATC1,²⁹ MAPK14 (P38),^{30,31} and FOS^{32,33} in cultured CsA-exposed neurons and dissociated trigeminal neurons (Fig. 4G). These genes are specific to CsA mechanism of action.^{29–33} Additionally, we analyzed the expression of GAP43, a proto-

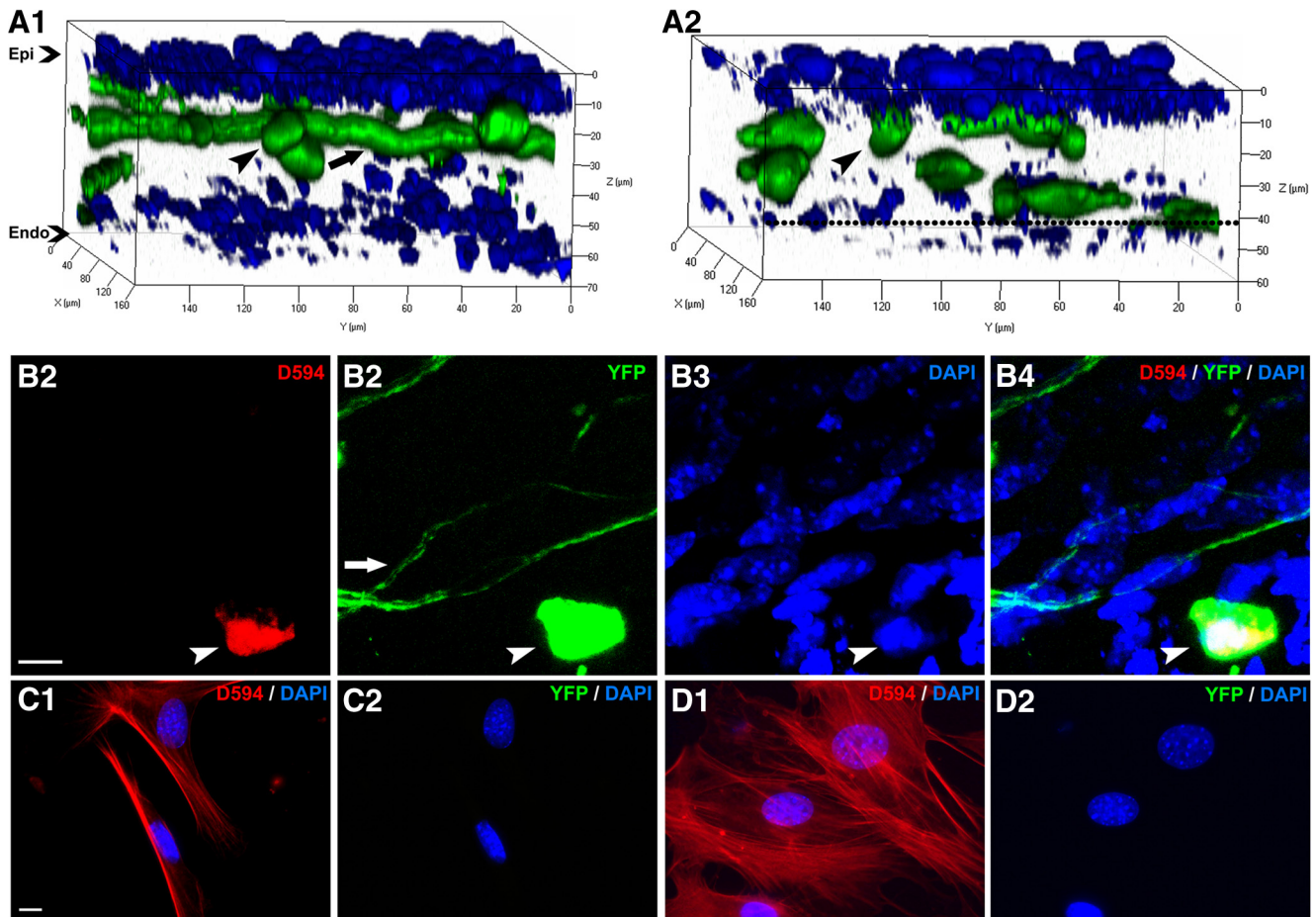


FIGURE 2. YFP fluorescent inflammatory cells in the cornea. (**A1**, **A2**) Three-dimensional reconstructed images of a *thy1*-YFP whole-mount cornea showing YFP+ nerves and cells (green) and DAPI-stained nuclei of epithelial and stromal cells (blue). The arrow points toward a stromal nerve and the arrowhead toward a YFP fluorescent inflammatory cell. In **A2**, the flap interface is shown in the black dotted line. Confocal images were taken 3 days after lamellar corneal surgery in the peripheral cornea just outside the flap edge (**A1**) and in the central cornea over the flap (**A2**). Note that YFP-positive cells are present along the stromal nerves in the anterior stroma of the corneal periphery (**A1**). In the corneal center (**A2**), nerves are absent and YFP-positive cells are present in both the anterior and posterior stroma (in the vicinity of the flap interface). (**B1**–**B4**) Whole-mount immunofluorescent staining of cornea showing that YFP fluorescent cells are T cells. Arrowhead points toward a YFP fluorescent inflammatory cell (**B2**, green) that shows positive staining with $\gamma\delta$ T-cell receptor antibody (**B1**, red). The cell nucleus stains with DAPI (**B3**, blue). (**C**, **D**) Immunofluorescent staining of cultured activated keratocytes (fibroblasts and myofibroblasts) showing that these cells are not YFP fluorescent. Corneal stromal fibroblasts (**C1**, **C2**) and myofibroblasts (**D1**, **D2**) show positive staining with α -smooth muscle actin antibody (red), but do not show YFP fluorescence (**C2**, **D2**, blue). The cell nucleus stains with DAPI (**C2**, **D2**, blue). White scale bar, 10 μ m.

type regeneration-associated gene.³⁴ CsA exposure significantly decreased the expression of NFATC1 and MAPK14 (P38) but significantly increased the expression of FOS (*c-fos*) and GAP43 ($P < 0.05$).

DISCUSSION

This study yielded four findings. (1) Lamellar corneal surgery induces a significant influx of inflammatory cells that peaks at postoperative day 3 and regresses thereafter. These inflammatory cells include YFP+ $\gamma\delta$ T cells that have been previously reported to promote corneal nerve regeneration after epithelial wounds.¹⁶ (2) CsA immunomodulation reduces corneal inflammation, as evidenced by significantly fewer YFP-positive cells and significantly reduced expression of IL6. (3) Use of 0.05% CsA twice daily for 6 weeks significantly retards regeneration of transected nerves. (4) In compartmental cultures of dissociated trigeminal neurons, CsA (5 μ g/mL, 24 hours) significantly impedes axonal growth, suggesting that in addition to immunomodulatory actions, CsA directly affects neurite growth. Together, these in vivo and in vitro findings suggest that cor-

neal inflammation normally accompanying nerve regeneration facilitates axonal growth. In the current investigation, a long duration (6 weeks) of CsA immunomodulation did not promote nerve regeneration. The study was terminated at 6 weeks because, in *thy1*-YFP+ mice, corneal nerve regeneration peaks between 4 and 6 weeks after nerve transection surgery, with no significant increase in nerve density occurring after 6 weeks.³⁵ Since we did not investigate whether blunting only the initial rapid influx of cells in the cornea is beneficial or detrimental to regenerating nerves, additional investigations are needed to clarify whether short-duration immunomodulation therapy is beneficial (limited to the first 1 to 2 weeks after surgery). Our goal in this study was to determine the neuronal effect of modulating inflammation that accompanies uncomplicated healing. For this reason, we excluded corneas that developed scar or vascularization as a result of infection or postoperative trauma. Our data should not be extrapolated to nerve regeneration in the setting of corneal healing complicated by excessive inflammation.

Li et al.¹⁶ recently reported that nerve regeneration is positively influenced by the inflammatory process after cor-

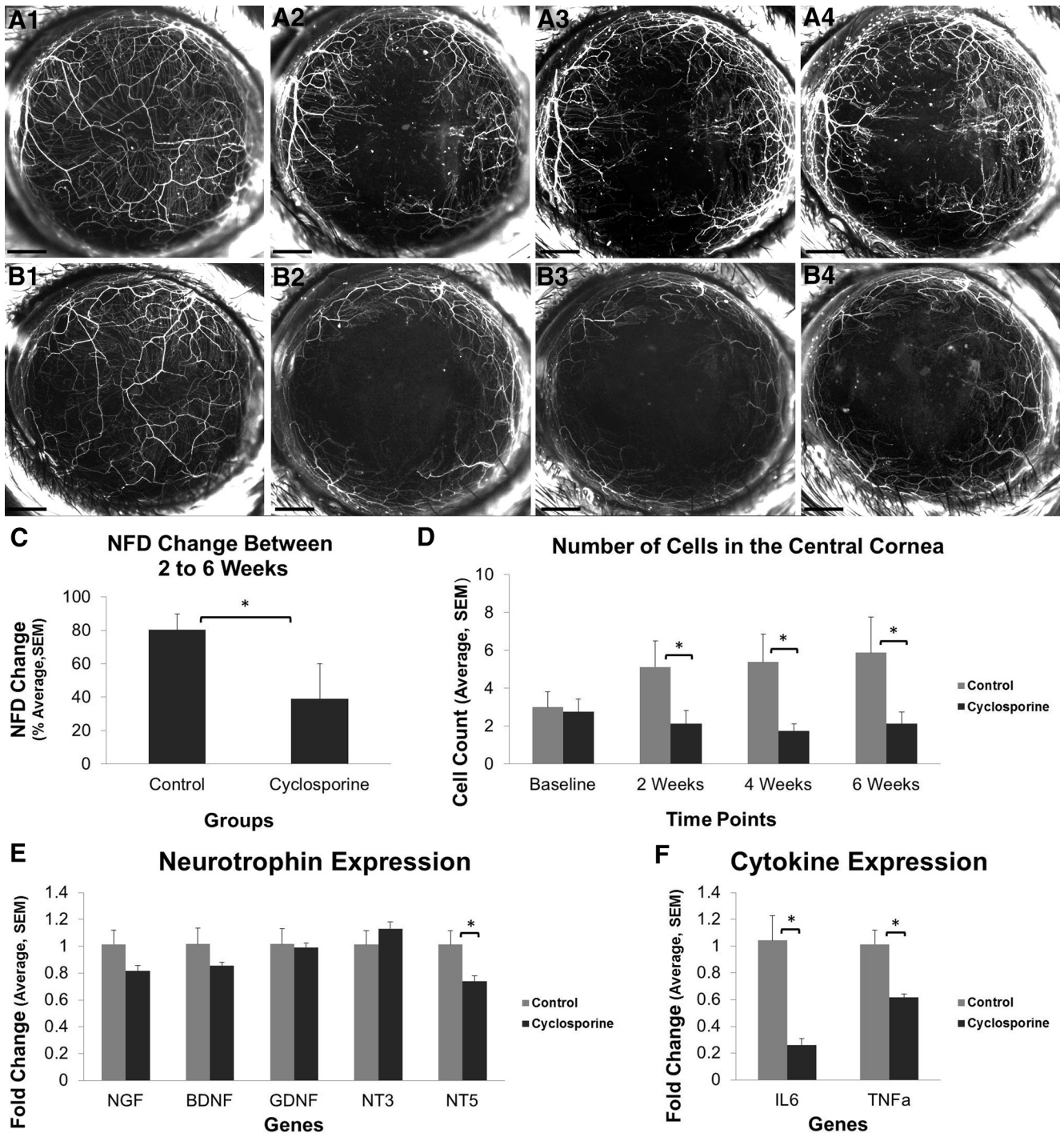


FIGURE 3. Effect of CsA on nerve regeneration after lamellar corneal surgery. (A1–B4) Serial in vivo maximum intensity projection images of fluorescent nerves and inflammatory cells in a *thy1-YFP* mouse cornea before surgery (A1, B1) and 2 weeks (A2, B2), 4 weeks (A3, B3), and 6 weeks (A4, B4) after surgery. Eyes were treated with artificial tears (A1–A4) or CsA (B1–B4) twice daily for 6 weeks. The NFD growth between weeks 2 and 6 (C) as well as the number of YFP-positive cells in the central 2-mm cornea (D) are significantly lower in the CsA group. Neurotrophin expression (E) and inflammatory cytokine expression (F) at 6 weeks. Scale bar, 500 μ m; * $P < 0.05$.

neal epithelial abrasion, a superficial injury that likely transects only epithelial and subbasal nerves. We performed lamellar corneal surgery and found that regenerative sprouting from proximal ends of transected stromal nerve trunks is also influenced by the inflammatory process. Several ophthalmic surgical procedures such as corneal transplants, LASIK, and cataract surgery require incisions to be placed in the cornea. These incisions will transect stromal corneal

nerves. If a main stromal trunk in the corneal periphery is transected, phenomenologic events of nerve regeneration, as reported here, can be reasonably expected to follow. The most direct practical implication of our results, from the narrow perspective of nerve regeneration alone, is that avoiding long-duration immunomodulation or anti-inflammatory treatment may benefit corneal reinnervation if the post-operative healing is uncomplicated.

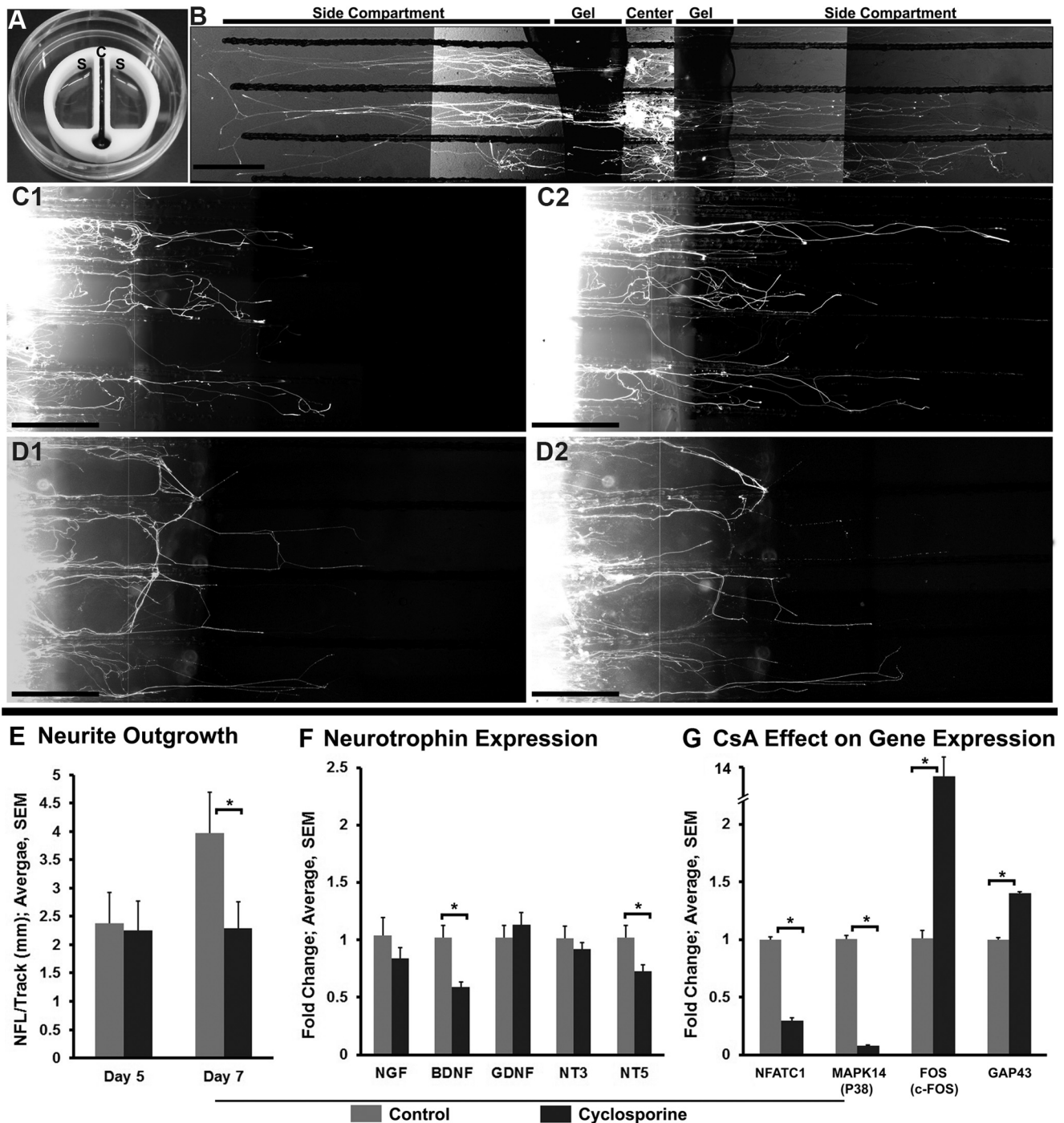


FIGURE 4. Effect of CsA on neurite outgrowth in compartmental cultures of dissociated trigeminal ganglion cells. (A) A device (Teflon) used for compartmental cultures of trigeminal ganglion neurons. The central compartment, which contains trypan blue dye, is isolated from side compartments containing culture media. Note the absence of leakage of the dye from the central compartment to the side compartments. (B) Fluorescent image showing neurites in the growth media. The cell bodies are isolated in the central compartment and the neurites extend into the side compartment parallel to the tracks. (C1–D2) Comparison of outgrowth between neurites exposed to vehicle (C1, C2) or CsA (D1, D2) for 24 hours. Neurite outgrowth was assessed on day 5 (C1, D1) before, and day 7 (C2, D2) after vehicle or CsA treatment. (E) Quantification of neurite outgrowth. The bars show the NFL per track before (day 5) and after (day 7) vehicle or CsA treatment. (F) Real-time qPCR analysis at day 7 shows that BDNF and NT5 gene expressions are significantly less after CsA treatment compared with vehicle treatment. (G) Real-time qPCR analysis of expression of genes that are specific to CsA mechanism of action (NFATC1, MAPK14, and FOS). Graph shows fold increase or decrease in gene expression in CsA-exposed neurons compared with gene expression in dissociated trigeminal neurons (control). CsA exposure significantly decreases the expression of NFATC1 and MAPK14 (P38) but significantly increases the expression of FOS (*c-fos*) and GAP43. * $P < 0.05$. Scale bar, 500 μm .

The inflammatory response in the cornea is complex, consisting of infiltration of inflammatory cells of heterogeneous lineages, activation of resident corneal cells, increased activity

of metalloproteinases, and elevated levels of inflammatory cytokines such as IL-1, IL6, IL-8, and TNF- α .^{36–42} Our study does not dissect the relative contribution of these various factors

toward promoting or retarding nerve regeneration. Instead, it is concentrated on the investigation of neuronal effects of inhibiting inflammation using a clinically relevant immunomodulating drug. We chose to investigate the expression of IL6 rather than other inflammatory cytokines for two reasons. First, the primary mechanism of CsA action involves regulation of T-cell activation through calcineurin, a major regulator of IL6 expression.⁴³⁻⁴⁵ Second, IL6 has independent neuronal actions and promotes nerve regeneration.⁴⁶⁻⁴⁸ We found that, corneal expression of both IL6 and TNF- α were reduced by CsA, more so with the former than with the latter. Similarly, Keller et al. reported that CsA inhibits IL6 more than TNF- α in skeletal muscle cell cultures.⁴⁹

Topical corticosteroids and CsA are the anti-inflammatory agents of choice for the management of most immune-mediated diseases of the ocular surface.^{42,50-52} In this study, we used CsA because the anti-inflammatory effects of topical CsA in vivo are mediated predominantly through its inhibitory effect on immune cells, primarily T cells. Unlike corticosteroids, CsA does not have a significant direct anti-inflammatory effect on the resident corneal cells. Therefore, our use of CsA minimizes interference with the corneal epithelium and keratocyte function as well as wound healing events. The pharmacologic action of CsA is mediated by its binding to cyclophilin, which inhibits the phosphatase calcineurin. CsA is approved by the FDA to treat dry eye disease. It is also used to treat other ocular surface disorders that may have an immune-based inflammatory component such as post-LASIK dry eye, contact lens intolerance, atopic keratoconjunctivitis, graft-versus-host disease, and herpetic stromal keratitis.⁵³ Our in vivo data suggest that CsA has neuronal actions. The inhibiting actions could be attributed, in part, to the reduced expression of proinflammatory, neurogenic cytokines such as IL6.

Our in vitro data show that CsA directly affects axonal growth. Two explanations could account for this direct effect. First, CsA may affect neurite outgrowth through downregulation of neurotrophins. We found that CsA treatment was associated with reduced expression of BDNF (in vitro) and NT5 (in vivo and in vitro). In the in vitro experiments, CsA was added to only the axonal compartment, and the trigeminal neuronal cells were the only source of BDNF and NT5. These findings suggest that CsA directly influences neurotrophin mRNA expression in neurons. Consistent with this idea, chronic administration of CsA has been shown to downregulate BDNF and its receptor tyrosine kinase receptor B in the brain.²⁸ An alternative explanation for a direct CsA effect on neurite growth in vitro is neurotoxicity. McDonald and colleagues⁵⁴ have reported that neuronal cultures exposed to 1 to 20 μ M CsA for 24 to 48 hours develop concentration-dependent neuronal death, with most neurons being destroyed by 20 μ M CsA. In our in vitro study, we used a 5 μ g/mL concentration of CsA (equivalent to approximately 5 μ M). In the study reported by McDonald et al.,⁵⁴ a 24-hour exposure to 5 μ M CsA did not induce neuronal death. Therefore, the concentration we used should be sublethal to neurons. In addition, in our compartmental culture method, the axons in the side compartment were exposed to CsA, whereas the neuronal cell bodies were in the central compartment, fluidically isolated from CsA. The rationale for performing compartmental culture was to mimic the in vivo corneal environment. The neuronal cell bodies reside in the trigeminal ganglion and only the trigeminal axons innervate the cornea. By avoiding direct contact of CsA with neuronal cell bodies, we expected to have further limited direct toxicity. Our results show that CsA exposure significantly decreases the expression of NFATC1 and MAPK14 but significantly increases the expression of FOS and GAP43. These data are in conformity with prior reported data on changes in gene expression due to

CsA.²⁹⁻³³ Given the changes in the expression of genes that are CsA action specific as well as significant expression of regeneration-associated gene GAP43,³⁴ our observed CsA effects on the neuronal growth are likely due to the specific effects of CsA and not cytotoxicity.

In humans, activated keratocytes (fibroblasts and myofibroblasts) express *thy1*.⁵⁵ To determine whether corneal fibroblasts and myofibroblasts are fluorescent in *thy1*-YFP mice, we activated the keratocytes isolated from corneal stroma using fibroblast induction media and myofibroblast induction media. We did not observe YFP fluorescence either in fibroblasts or in myofibroblasts in vitro (data not shown). We immunostained fibroblasts and myofibroblasts with anti- α -smooth muscle actin antibody and DAPI (to visualize cells). Both cell phenotypes showed appropriate staining with anti- α -smooth muscle actin antibody and DAPI but were not fluorescent in the YFP wavelength. By use of an identical immunostaining protocol, cultured trigeminal neurons were shown to be YFP fluorescent and stained with specific neuronal antibodies (data not shown). Further, in whole-mount confocal immunofluorescent microscopy we observed YFP fluorescence only in $\gamma\delta$ T cells, but the surrounding stromal cells were not YFP fluorescent. Taken together, these experiments reveal that, in *thy1*-YFP transgenic mice, corneal stromal cells (resident or activated) are not fluorescent.

In conclusion, using in vivo and in vitro methods, we found that prolonged immunomodulation with CsA retards axonal growth of transected corneal nerves. This suggests that inflammation that accompanies uncomplicated healing facilitates neurite growth.

Acknowledgments

The authors thank Ke Ma, PhD, for help with confocal imaging and 3D reconstruction.

References

1. Terenghi G. Peripheral nerve regeneration and neurotrophic factors. *J Anat.* 1999;194:1-14.
2. Schmitt AB, Breuer S, Liman J, et al. Identification of regeneration-associated genes after central and peripheral nerve injury in the adult rat. *BMC Neurosci.* 2003;19:4-8.
3. Dahlin LB. Stimulation of regeneration of the sciatic nerve by experimentally induced inflammation in rat. *Scand J Plast Reconstr Surg Hand Surg.* 1992;26:121-125.
4. Yong VW. Inflammation in neurological disorders: a help or a hindrance? *Neuroscientist.* 2010;16:408-420.
5. Popovich PG, Jones TB. Manipulating neuroinflammatory reactions in the injured spinal cord: back to basics. *Trends Pharmacol Sci.* 2003;24:13-17.
6. Schwartz M, Moalem G, Leibowitz-Amit R, Cohen IR. Innate and adaptive immune responses can be beneficial for CNS repair. *Trends Neurosci.* 1999;22:295-299.
7. Jones TB, Ankeny DP, Guan Z, et al. Passive or active immunization with myelin basic protein impairs neurological function and exacerbates neuropathology after spinal cord injury in rats. *J Neurosci.* 2004;24:3752-3761.
8. Hendrix S, Peters EM. Neuronal plasticity and neuroregeneration in the skin: the role of inflammation. *J Neuroimmunol.* 2007;184:113-126.
9. Gronert K. Review resolution, the grail for healthy ocular inflammation. *Exp Eye Res.* 2010;91:478-485.
10. Zhang M, Chen J, Luo L, Xiao Q, Sun M, Liu Z. Altered corneal nerves in aqueous tear deficiency viewed by in vivo confocal microscopy. *Cornea.* 2005;24:818-824.
11. Benítez-del-Castillo JM, Wasfy MAS, Fernandez C, Garcia-Sanchez J. An in vivo confocal masked study on corneal epithelium and subbasal nerves in patients with dry eye. *Invest Ophthalmol Vis Sci.* 2004;45:3030-3035.

12. Benítez-del-Castillo JM, Acosta MC, Wassfi MA, et al. Relation between corneal innervations with confocal microscopy and corneal sensitivity with noncontact esthesiometry in patients with dry eye. *Invest Ophthalmol Vis Sci.* 2007;48:173-181.
13. Villiani E, Galimberti D, Viola F, et al. The cornea in Sjogren's syndrome: an in vivo confocal study. *Invest Ophthalmol Vis Sci.* 2007;48:2017-2022.
14. Tuisku IS, Konttinen YT, Konttinen LM, et al. Alterations in corneal sensitivity and nerve morphology in patients with primary Sjogren's syndrome. *Exp Eye Res.* 2008;86:879-885.
15. Tuominen ISJ, Konttinen YT, Vesaluoma MH, Moilanen JAO, Helinto M, Tervo TM. Corneal innervation and morphology in primary Sjogren's syndrome. *Invest Ophthalmol Vis Sci.* 2003;44:2545-2549.
16. Li Z, Burns AR, Han L, Rumbaut RE, Smith CW. IL-17 and VEGF are necessary for efficient corneal nerve regeneration. *Am J Pathol.* 2011;178:1106-1116.
17. Yoshida K, Gage FH. Cooperative regulation of nerve growth factor synthesis and secretion in fibroblast growth factor and other cytokines. *Brain Res.* 1992;569:14-25.
18. Hattori A, Tanaka E, Murase K, et al. Tumor necrosis factor stimulates the synthesis and secretion of biologically active nerve growth factor in nonneuronal cells. *J Biol Chem.* 1993;268:2577-2582.
19. Lee HK, Ryu IH, Seo KY, et al. Topical 0.1% prednisolone lowers nerve growth factor expression in keratoconjunctivitis sicca patients. *Ophthalmology.* 2006;113:198-205.
20. Haeryfar SM, Hoskin DW. Thy-1: more than a mouse pan-T-cell marker. *J Immunol.* 2004;173:3581-3588.
21. Yu CQ, Rosenblatt MI. Transgenic corneal neurofluorescence in mice: a new model for in vivo investigation of nerve structure and regeneration. *Invest Ophthalmol Vis Sci.* 2007;48:1535-1542.
22. Al-Aqaba MA, Alomar T, Miri A, Fares U, Otri AM, Dua HS. Ex vivo confocal microscopy of human corneal nerves. *Br J Ophthalmol.* 2010;94:1251-1257.
23. Beales MP, Funderburgh JL, Jester JV, Hassell JR. Proteoglycan synthesis by bovine keratocytes and corneal fibroblasts: maintenance of the keratocyte phenotype in culture. *Invest Ophthalmol Vis Sci.* 1999;40:1658-1663.
24. Malin SA, Davis BM, Molliver DC. Production of dissociated sensory neuron cultures and considerations for their use in studying neuronal function and plasticity. *Nat Protoc.* 2007;2:152-160.
25. Campenot RB, Lund K, Mok SA. Production of compartmented cultures of rat sympathetic neurons. *Nat Protoc.* 2009;4:1869-1887.
26. Pazyra-Murphy MF, Segal RA. Preparation and maintenance of dorsal root ganglia neurons in compartmented cultures (Online). *J Vis Exp.* 2008;20:951.
27. Gortzak R, Maftzir G, Aharonov O, Benezra D. Effect of cyclosporin A, rapamycin, and FK-506 on corneal epithelial cells and lymphocyte proliferation. *Ocul Immunol Inflamm.* 1993;1:203-209.
28. Chen CC, Hsu LW, Huang LT, Huang TL. Chronic administration of cyclosporine A changes expression of BDNF and TrkB in rat hippocampus and midbrain. *Neurochem Res.* 2010;35:1098-1104.
29. Miyazaki M, Fujikawa Y, Takita C, Tsumura H. Tacrolimus and cyclosporine A inhibit human osteoclast formation via targeting the calcineurin-dependent NFAT pathway and an activation pathway for c-Jun or MITF in rheumatoid arthritis. *Clin Rheumatol.* 2007;26:231-239.
30. Matsuda S, Koyasu S. Mechanisms of action of cyclosporine. *Immunopharmacology.* 2000;47:119-125.
31. Matsuda S, Koyasu S. Regulation of MAPK signaling pathways through immunophilin-ligand complex. *Curr Top Med Chem.* 2003;3:1358-1367.
32. Su Q, Eugster HP, Ryffel B, Dumont FJ. Cyclosporin A enhances the calcium-dependent induction of AP-1 complex and c-fos mRNA in a T cell lymphoma. *Biochem Biophys Res Commun.* 1996;229:249-256.
33. Saggi SJ, Andoh TF, Safirstein R, Bennett WM. Cyclosporin induces renal proto-oncogene RNA message and increased transforming growth factor-beta prior to renal fibrosis: modification by calcium channel blockade in the salt replete rat. *Nephrology (Carlton).* 2004;9:58-64.
34. Martin RE, Bazan NG. Growth-associated protein Gap43 and nerve cell adhesion molecule in sensory nerves of cornea. *Exp Eye Res.* 1992;55:307-314.
35. Namavari A, Chaudhary S, Sarkar J, et al. In vivo serial imaging of regenerating corneal nerves after surgical transection in transgenic thy1-YFP mice. *Invest Ophthalmol Vis Sci.* 2011;52:8025-8032.
36. Brignole F, Pisella PJ, Goldschild M, et al. Flow cytometric analysis of inflammatory markers in conjunctival epithelial cells of patients with dry eyes. *Invest Ophthalmol Vis Sci.* 2000;41:1356-1363.
37. Stern ME, Gao J, Schwab TA, et al. Conjunctival T-cell subpopulations in Sjögren's and non-Sjögren's patients with dry eye. *Invest Ophthalmol Vis Sci.* 2002;43:2609-2614.
38. Pflugfelder SC, Jones D, Ji Z, et al. Altered cytokine balance in the tear fluid and conjunctiva of patients with Sjogren's syndrome keratoconjunctivitis sicca. *Curr Eye Res.* 1999;19:201-211.
39. Solomon A, Dursun D, Liu Z, et al. Pro- and anti-inflammatory forms of interleukin-1 in the tear fluid and conjunctiva of patients with dry eye disease. *Invest Ophthalmol Vis Sci.* 2001;42:2283-2292.
40. Smith VA, Rishmawi H, Hussein H, et al. Tear film MMP accumulation and corneal disease. *Br J Ophthalmol.* 2001;85:147-153.
41. Marsh P, Pflugfelder SC. Topical nonpreserved methylprednisolone therapy for keratoconjunctivitis sicca in Sjogren's syndrome. *Ophthalmology.* 1999;106:811-816.
42. Sall K, Stevenson OD, Mundorf TK, et al. Two multicenter, randomized studies of the efficacy and safety of cyclosporine ophthalmic emulsion in moderate to severe dry eye disease. CSA Phase 3 Study Group. *Ophthalmology.* 2000;107:631-639.
43. Halloran PF, Kung L, Noujaim J. Calcineurin and the biological effect of cyclosporine and tacrolimus. *Transplant Proc.* 1998;30:2167-2170.
44. Banzet S, Koulmann N, Sanchez H, et al. Contraction-induced interleukin-6 transcription in rat slow-type muscle is partly dependent on calcineurin activation. *J Cell Physiol.* 2007;210:596-601.
45. Banzet S, Koulmann N, Simler N, et al. Fibre-type specificity of interleukin-6 gene transcription during muscle contraction in rat: association with calcineurin activity. *J Physiol.* 2005;566:839-847.
46. Lara-Ramírez R, Segura-Anaya E, Martínez-Gómez A, Dent MA. Expression of interleukin-6 receptor alpha in normal and injured rat sciatic nerve. *Neuroscience.* 2008;152:601-608.
47. Galiano M, Liu ZQ, Kalla R, et al. Interleukin-6 (IL6) and cellular response to facial nerve injury: effects on lymphocyte recruitment, early microglial activation and axonal outgrowth in IL6-deficient mice. *Eur J Neurosci.* 2001;14:327-341.
48. Zhong J, Dietzel ID, Wahle P, Kopf M, Heumann R. Sensory impairments and delayed regeneration of sensory axons in interleukin-6-deficient mice. *J Neurosci.* 1999;19:4305-4313.
49. Keller C, Hellsten Y, Steensberg A, Pedersen BK. Differential regulation of IL6 and TNF- α via calcineurin in human skeletal muscle cells. *Cytokine.* 2006;36:141-147.
50. Foster CS. Immunologic disorders of the conjunctiva, cornea, and sclera. In: Albert DM, Jakobiec FA, eds. *Principles and Practice of Ophthalmology.* 2nd ed. Philadelphia, PA: WB Saunders; 2000: 803-828.
51. Dana MR, Qian Y, Hamrah P. Twenty-five year panorama of corneal immunology. *Cornea.* 2000;19:625-643.
52. Leibowitz HM, Kupferman A. Antiinflammatory medications. *Int Ophthalmol Clin.* 1980;20:117-134.
53. Donnenfeld E, Pflugfelder SC. Topical ophthalmic cyclosporine: pharmacology and clinical uses. *Surv Ophthalmol.* 2009;54:321-338.
54. McDonald JW, Goldberg MP, Gwag BJ, Chi SI, Choi DW. Cyclosporine induces neuronal apoptosis and selective oligodendrocyte death in cortical cultures. *Ann Neurol.* 1996;40:750-758.
55. Pei Y, Sherry DM, McDermott AM. Thy-1 distinguishes human corneal fibroblasts and myofibroblasts from keratocytes. *Exp Eye Res.* 2004;79:705-712.